An Experimental Study of Flux-Linkage Relations in a Synchronous Generator at Steady States

AUTHOR(S):

UEDA, Yoshisuke; HIKIHARA, Takashi; UENOSONO, Chikasa

An Experimental Study of Flux-Linkage Relations in a Synchronous Generator at Steady States

By

Yoshisuke UEDA*, Takashi HIKIHARA* and Chikasa UENOSONO**

(Received December 26, 1985)

Abstract

The inductances of a synchronous generator at a three-phase balanced synchronous operation are discussed experimentally by measuring the air-gap flux-density distributions. The results revealed general aspects of inductances, which depend on the operating conditions of the generator. In particular, the appearance of a unilateral inductance from the armature to the field windings is noteworthy. Special attention is also directed towards the relations between the magnetic flux-linkages and the currents of the armature and the field windings. As a result of this investigation, an alteration is proposed for a conventianal, field flux-linkage relation. The alteration has not been reported hitherto and can not be derived from the conventional theory of synchronous machines.

1. Introduction

Synchronous generators play the most important role on an electric power system, and to grasp their exact characteristics is essential for the proper operation of the system. At intervals over a period of about a century numerous papers have reported on these subjects, and at present the theory of synchronous machines seems to be recognized as if it was completed[1].

In the theory of synchronous machines, the effects of saturation and hysteresis are generally neglected, and linear relations have been used between the magnetic fluxes and currents. Because these effects are considered as small in a large number of machines, the average value of each of the coefficients is regarded to be a rather constant quantity. In those cases when consideration of the effects of saturation and hysteresis becomes necessary, correction coefficients are usually introduced in order to represent the deviation from the corresponding quantities. At first sight, the above point of view seems to be natural. However, we meet with an experimental fact that is inconsistent with the conventional theory.

* Department of Electrical Engineering II.
** Emeritus professor of Kyoto University.

In this paper, inductances of a synchronous generator at a three-phase balanced synchronous operation are discussed experimentally. At first, by using search coils placed at the tooth tips of the armature we measure the air-gap flux-density distributions for various loading conditions of the generator. Later, the flux-linkages are evaluated by integrating the air-gap flux-density distributions, and the relations between the flux-likages and the currents are examined quantitatively. As a result of this investigation, we propose an alteration to the conventional relation between field flux-linkages and currents of field and armature windings. Admitting that the tested generator has somewhat special structures, the alteration is considered to be applicable to a large number of machines. It may exhibit a universal property of synchronous machines which has not been reported hitherto.

2. Outline of Experiment

2.1. Tested generator

The tested generator is a four salient-pole generator. The ratings and dimensions of the tested generator with nomenclatures are given in Table 1. The locations of the search coils at the armature tooth tips and various parts of the rotor are shown in Fig. 1. The damper windings of the tested generator can be attached and detached freely. In the present experiment, all the damper windings are detached from the tested generator.

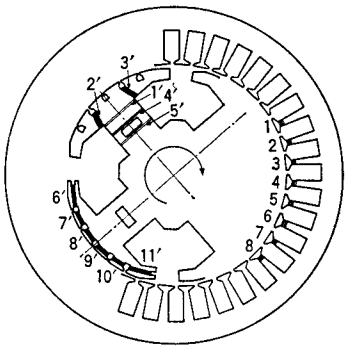

Fig. 1. A cross section of the synchronous generator and disposition of the search coils.

This tested generator was designed to simulate a 13 (MVA) generator in a 154 (kV) system. In order to provide it with the similar no-load saturation characteristics and the same short-circuit ratio as in real machines, isthmus field cores are adopted. The nominally induced electromotive force of the tested generator is 220 (V) at a field current of $i_f=3.2$(A). The no-load saturation characteristics will be shown in Fig. 7, Sec. 4.1.

Table 1. Ratings and Dimensions of Tested Generator.

Rating
Number of phase: 3, Frequency: 60(Hz), Number of poles: 4
Output power: 6(kVA), $\cos\phi$: 0.9(lagging), Rating: Continuous,
Rated Voltage: 220(V), Rated load current: 15.7(A),
Number of revolutions: 1800(rpm), Field current: 4.8(A)
Stator
Diameter: Inside diameter 275(mm) (r=137.5(mm)), Outside diameter 410(mm),
Core length: l=130(mm), Actual air-gap in pole center: 3.3(mm)
Number of slot: 36
Number of slots per pole per phase: 3
Skew: 24(mm) at 275 ϕ
Number of series conductors: 8
Stator (machine) slot pitch: $\alpha_m=2\pi/36$(rad)
Stator (electrical) slot pitch: $\alpha=2\pi/18$(rad)
Armature windings: lap, double, distributed, short-pitch, integral slot windings and star connected
Dc resistance of armature winding at 75°C: r_a=0.149(Ω)
Number of turns of search coil: N=3
Rotor
Rotor diameter: 268.4(mm)
Core length: 130(mm)
Axial length of pole head: 90(mm)
Angular width of pole arc: 76.6(deg)
Laminated poles
Miled steel 1.6(mm)
Number of turns of field winding per pole: N_f=500
Dc resistance of field windings: 14.9(Ω)

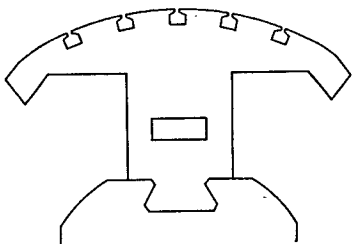

2.2. Experimental system and setup conditions

The experimental system is shown in Fig. 2, which is the so-called single generator operating onto an infinite bus system. In Fig. 2, the transformer *Tr.* 1 has the following ratings: 6(kVA), primary/secondary voltages 220/3300(V), and the *Tr.* 2: 20 (kVA), 3300/210 (V). We used the transmission line with impedance 40 (%)

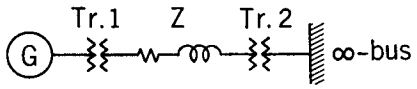

Fig. 2. Single generator operating onto an infinite bus system.

(based on 220(V) and 15.7(A)) and the distribution system source 210(V), 60(Hz) as an infinite bus.

The tested generator is driven by a separately excited dc-motor with the rating 15(kW) by the following two ways:

(1) Keeping the field current constant ($i_f=2.0$, 3.2, 5.0(A)), the output power of the generator is increased quasi-statistically in the steady-state stability region.

(2) Keeping the generator output power constant ($P=6.0$(kW)), the field current is decreased in the same way in the same region.

We will see the steady-state stability region in Fig. 9, Sec. 4.1, where the measured points are shown by small circles.

3. Flux-Based Calculation of Inductances

In this section, we give the method of calculation of inductances by using search coils at the armature tooth tips.

3.1. Air-gap flux-density distribution

This tested generator is represented by a two salient pole generator as shown in Fig. 3. The coordinate of the air-gap is denoted by ξ (rad), and the origin of

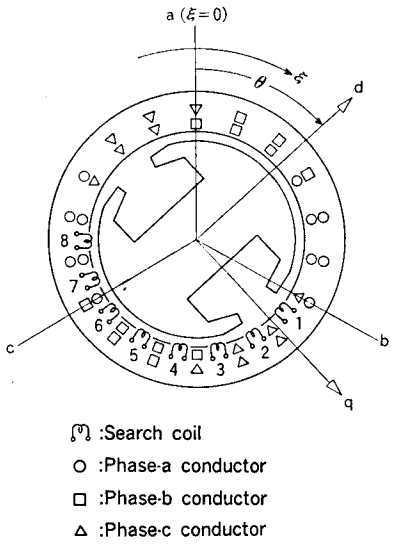

Fig. 3. Disposition of conductors of each phase and variable ξ expressing the air-gap location and θ the direct axis of rotor.

the coordinate is set at the axis of the phase-a armature winding. The positive direction coincides with that of the rotor rotation. The location of the rotor is denoted by θ (rad), which represents the angle of the direct axis of the rotor from the axis of the phase-a winding. Denoting the angular frequency of the infinite bus by $\omega(=120\pi$ (rad/sec)), θ is given by

$$\theta=\omega t+\delta \tag{1}$$

where δ (rad) is called a rotor angle.

By using these coordinates, the air-gap flux-density distribution $B(\xi,\ \theta)$ (Wb/m^2) can be expressed by[2]:

$$\begin{aligned}B(\xi,\ \theta)=&\sum_{n=1,3,5,\cdots}\{(B_n+B_{nd})\cos n(\xi-\theta)+B_{nq}\sin n(\xi-\theta)\}\\&+B_{5c}\cos(5\xi+\theta)+B_{5s}\sin(5\xi+\theta)\\&+B_{7c}\cos(7\xi-\theta)+B_{7s}\sin(7\xi-\theta)\end{aligned} \tag{2}$$

where B_n represents the no-load flux-density, B_{nd} and B_{nq} the direct and quadrature components of the armature reaction flux-density, which are stationary with respect to the poles. The terms containing B_{5c} and B_{5s} represent the 5 th space harmonic component which rotates in the opposite direction of the rotor at the speed of 1/5 of the rotor speed. The terms, B_{7c} and B_{7s}, represent the 7 th space harmonic component which rotates in the same direction as the rotor at the speed of 1/7 of the rotor speed. These components originate in the structure of the armature windings. They are not stationary with respect to the poles, and pulsate over the rotor at 6 times the fundamental frequency. However, they are time fundamental components with respect to the stator.

It should be remarked that the coefficients B's in Eq. (2) become constants at a three-phase balanced synchronous operation. On the other hand, they change with time at transient states and/or unbalanced-load operations.

Each component in Eq. (2) can be obtained by using the induced electromotive forces $e_{sc}(\xi_i,\ \theta)$ of the neighboring three search coils ($i=j,\ j+1,\ j+2$). That is, non-stationary components can be separated from stationary components. There is no room to give the detailed procedure here, but the important space and time fundamental component is given as follows[2]:

$$\left.\begin{aligned}B_1+B_{1d}&=\frac{1}{3\omega N r\alpha_m l}\sum_{i=j}^{j+2}\{E_{1c}(\xi_i)\sin\xi_i-E_{1s}(\xi_i)\cos\xi_i\}\\B_{1q}&=\frac{-1}{3\omega N\alpha r_m l}\sum_{i=j}^{j+2}\{E_{1c}(\xi_i)\cos\xi_i+E_{1s}(\xi_i)\sin\xi_i\}\end{aligned}\right\} \tag{3}$$

where

$$\left.\begin{aligned}E_{1c}(\xi_i)&=\frac{1}{\pi}\int_0^{2\pi}e_{sc}(\xi_i,\ \theta)\cos\theta\,d\theta\\E_{1s}(\xi_i)&=\frac{1}{\pi}\int_0^{2\pi}e_{sc}(\xi_i,\ \theta)\sin\theta\,d\theta\end{aligned}\right\} \tag{4}$$

In the following expression, we exclude the non-stationary components in Eq. (2) because they have no essential effect on the generator characteristics. Instead of Eq. (2), we sometimes use the abbreviated expression of the air-gap flux-density distribution:

$$B(\eta)=\sum_{n=1,3,5,\cdots}\{(B_n+B_{nd})\cos n\eta+B_{nq}\sin n\eta\} \tag{5}$$

where $\eta=\xi-\theta$ represents the coordinate of the air-gap standing on the rotor.

3.2. Flux-based inductances of armature windings

The flux-linkage of the phase-a armature winding $\psi_a(\theta)$ (Wb) can be derived by integrating $B(\xi,\ \theta)$ over the area of the phase-a winding. The result is as follows[2]:

$$\psi_a(\theta)=\sum_{n=1,3,5,\cdots}K_n\{(B_n+B_{nd})\cos n\theta-B_{nq}\sin n\theta\} \tag{6}$$

where

$$K_n=\frac{32rl_e}{n^2\alpha}\left(\sin\frac{n\pi}{2}\right)(\sin n\alpha+\sin 2n\alpha) \tag{7}$$

$l_e=\kappa_e l$: effective axial length of armature

(κ_e : coefficient)

From the symmetry of the machine structure, we obtain

$$\psi_b(\theta)=\psi_a(\theta-2\pi/3),\quad \psi_c(\theta)=\psi_a(\theta-4\pi/3) \tag{8}$$

In the following treatment we neglect the higher harmonics in Eqs. (6) and (8), because they have no essential effect on the steady-state balanced operation of generators. By applying the dq-transformation* to $\psi_a(\theta)$, $\psi_b(\theta)$ and $\psi_c(\theta)$, we have

$$\psi_d=K_1(B_1+B_{1d}),\quad \psi_q=K_1B_{1q} \tag{9}$$

In the flux-based discussion, the armature current $i_a(\theta)$, $i_b(\theta)$ and $i_c(\theta)$ should preferably be expressed by

$$\left.\begin{aligned} i_a(\theta)&=-\sqrt{2}I\sin(\theta+\gamma)\\ i_b(\theta)&=-\sqrt{2}I\sin(\theta+\gamma-2\pi/3)\\ i_c(\theta)&=-\sqrt{2}I\sin(\theta+\gamma-4\pi/3)\end{aligned}\right\} \tag{10}$$

where γ represents the phase difference between the no-load phase voltage and the armature current, and is called the internal power factor angle. In the same manner as in the flux-linkages, we have

$$i_d=-\sqrt{2}I\sin\gamma,\quad i_q=\sqrt{2}I\cos\gamma \tag{11}$$

We use the following conventional relations between the flux-linkages ψ_d, ψ_q and the currents i_f, i_d, i_q.

$$\left.\begin{aligned} \psi_d&=K_1(B_1+B_{1d})=L_{df}i_f-L_{ad}i_d\\ \psi_q&=K_1B_{1q}\qquad\quad =\qquad -L_{aq}i_q\end{aligned}\right\} \tag{12}$$

---

* $\psi_d=\frac{2}{3}\{\psi_a\cos\theta+\psi_b\cos(\theta-2\pi/3)+\psi_c\cos(\theta-4\pi/3)\}$

$\psi_q=-\frac{2}{3}\{\psi_a\sin\theta+\psi_b\sin(\theta-2\pi/3)+\psi_c\sin(\theta-4\pi/3)\}$

where the L's are inductances to be defined later. The term $L_{df}i_f$ in Eq. (12) represents the direct component of the armature linkage due to the field mmf. The terms $L_{ad}i_d$ and $L_{aq}i_q$ are direct and quadrature components of the armature linkages. The appropriateness of the above relations was also observed in the extent of our previous experiment[2].

In order to determine the inductances we use the no-load value of B_1 to separate it from B_1+B_{1d}. Then we have the inductances of the armature windings as follows:

$$L_{df}=\frac{K_1B_1}{i_f},\quad L_{ad}=\frac{K_1B_{1d}}{-i_d},\quad L_{aq}=\frac{K_1B_{1q}}{-i_q} \tag{13}$$

It is supposed that the inductances thus obtained do not contain leakage components, because owing to the measuring method every flux-line corresponding to the stationary components of $B(\eta)$ is considered to interlink with the armature windings.

In the practical calculation of the above inductances, a serious matter arises in the evaluation of the effective axial length of the armature windings l_e in Eq. (7). We will discuss this problem in the following section correlated with the leakage impedances of the armature windings.

3.3. Effective axial length and leakage impedance of armature windings

In the previous section we have pointed out the significance of the effective axial length of the armature windings. In the strict sense, it may change even at a balanced-load operation depending on the operating conditions of the generator. In this section, we try to evaluate it by using an air-gap flux-density distribution.

In order to explain the method of evaluation, it is convenient to use a vector diagram as shown in Fig. 4. In the figure, e_a represents the internal electromotive force, e_t terminal voltage and i_a armature current of a phase-a winding. The vector quantities e_t and i_a can be measured easily, whereas we can get e_a directly only for a no-load operation. At on-load operation e_a cannot be measured but can be derived by an air-gap flux-density distribution so far as the effective axial length of armature l_e is given beforehand. That is,

$$e_a(\theta)=\frac{d\psi_a(\theta)}{dt}=-\omega K_1\{B_{1q}\cos\theta+(B_1+B_{1d})\sin\theta\} \tag{14}$$

where

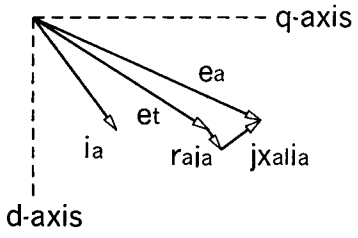

Fig. 4. Vector diagram.

$$K_1=\frac{32rl_e}{\alpha}(\sin\alpha+\sin 2\alpha)\equiv Kl_e$$

Let us here denote the leakage impedance of armature windings by r_a+jx_{al}, and regard the value of r_a as a measured one 0.149(Ω) obtained by the Bridge Method (converted value at 75°C). Then the vector quantities e_t, i_a, $r_a i_a$ are known. As for the e_a and $jx_{al}i_a$ their directions are known but their magnitudes are unknown. Referring again to Fig. 4, one may see that the magnitudes e_a and $jx_{al}i_a$ are easily determined by their intersection. Thus regarding l_e and x_{al} as unknown quantities, we obtain the following simultaneous equation:

$$\left.\begin{aligned} e_{td}+r_a i_d-x_{al}i_q&=\omega Kl_e B_{1q}\\ e_{tq}+r_a i_q+x_{al}i_d&=\omega Kl_e(B_1+B_{1d})\end{aligned}\right\} \tag{15}$$

where e_{td} and e_{tq} are the dq-transformed terminal voltages of the armature windings.

3.4. Flux-based inductances of field windings

We have discussed the inductances of armature windings by using an air-gap flux-density distribution. As armature windings are situated facing the air-gap, their flux-linkages are easily evaluated. In the salient type tested generator, however, the evaluation of field flux-linkages is not so easy since field windings are provided apart from the air-gap. Therefore, in order to estimate field linkages by using an air-gap flux-density distribution, it is required to make the flux path clear in the generator.

We have already reported in Ref. 3 that, when the output power of the generator increases, the flux distributions in the generator become complicated, and there appear so-called aa-loop flux components, which pass through the pole faces but do not interlink with the field windings. Let us here briefly explain these components as well as the ordinary, so-called af-loop flux components.

Figure 5(a) shows an air-gap flux-density distribution for a comparatively small armature current ($i_f=3.2$(A), $P=2.0$(kW)). Based on this distribution, a schematic flux-line behavior inside the generator is constructed in Fig. 5(b). In the figure, the direction of the magnetic flux is reversed at zero point η_0 where $B(\eta_0)=0$ and the branching point η_c, determined by

$$\int_{\eta_0-\pi}^{\eta_c}B(\eta)d\eta=\int_{\eta_c}^{\eta_0}B(\eta)d\eta \tag{16}$$

divides the total flux into the right and left portions. In this case, all flux-lines passing through the air-gap interlink with the armature and the field winding, and we call them af-loop flux components.

Figures 6(a) and (b) show the case for a relatively large armature current ($i_f=3.2$(A), $P=7.4$(kW)). As shown in the figure, the flux-lines passing through the air-gap interval between point η_1 and η_2 do not interlink with the field windings. Thus, aa-loop flux components appear. At point η_3, the flux flow branches into two

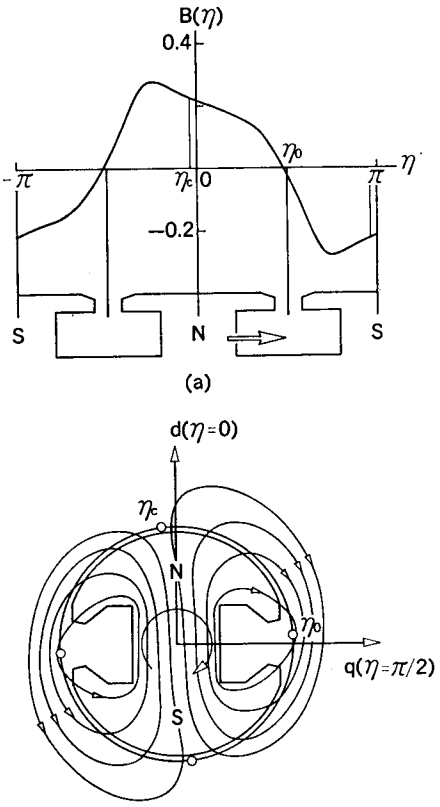

(a) Air-gap flux-density distribution
(b) Flux-line behavior inside the generator

Fig. 5. Situations for the case of relatively light load operation (i_f=3.2(A), P=2.0(kW)).

parts, one to pole N and the other to pole S. Point η_2 is determined presumably by either the local maximum value of $B(\eta)$ or the edge of the pole (η_p=76.6°. (See Table 1)[2]). Point η_1 in Fig. 6 is calculated by the following equation:

$$\int_{\eta_1}^{\eta_0} B(\eta)d\eta = -\int_{\eta_0}^{\eta_2} B(\eta)d\eta \tag{17}$$

The square on the flux-line in Fig. 6(b) passing through points η_1 and η_2 shows a singular (saddle) point of the magnetic field. From the feature of the air-gap flux-density distribution in Fig. 6(a), the existence of a saddle point can be deduced but the location cannot be settled exactly.

Based on the above discussion, the flux-linkage of the field windings ψ_f(Wb) can be derived by integrating $B(\eta)$ over the af-loop flux range. The result is as follows:

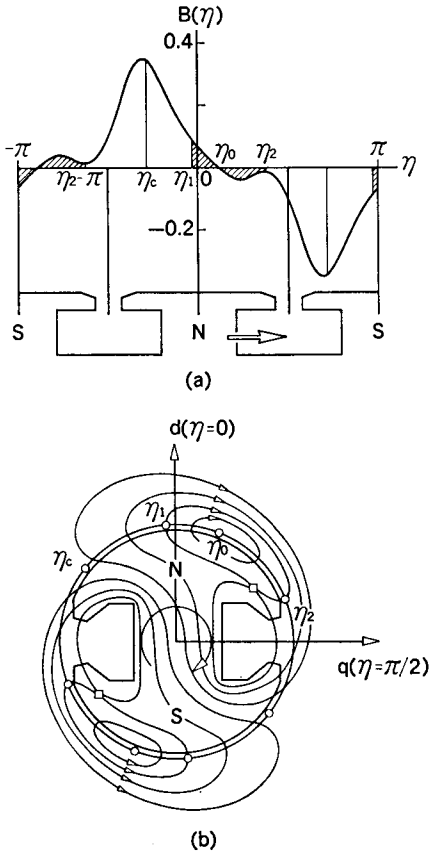

(a) Air-gap flux-density distribution
(b) Flux-line behavior inside the generator

Fig. 6. Situations for the case of relatively heavy load operation ($i_f=3.2$(A), $P=7.4$(kW)).

$$\begin{aligned}\psi_f &= 2N_f l_e \int_{\eta_2-\pi}^{\eta_1} B(\eta) r d\eta \\ &= \sum_{n=1,3,5,\cdots} K_{fn}\{(B_n+B_{nd})(\sin n\eta_1+\sin n\eta_2) \\ &\quad -B_{nq}(\cos n\eta_1+\cos n\eta_2)\}\end{aligned} \tag{18}$$

where

$$K_{fn}=\frac{2N_f r l_e}{n}$$

By putting $\eta_1=\eta_2=\eta_0$, this relation is also applicable to the case when there is no aa-loop component. It is to be noted that the field linkages thus obtained do not contain the field-leakage components.

Contrary to the conventional equation, we suggest the following relation between the field flux-linkage ψ_f and the currents i_f, i_d, i_q.

$$\psi_f = L_f i_f - \frac{3}{2} L_{fd} i_d + \frac{3}{2} L_{fq} i_q \tag{19}$$

where the L's are inductances to be defined later. This proposition is based on the fact that the components B_n, B_{nd}, B_{nq} of air-gap flux-densities are mainly dependent only on i_f, i_d, i_q, respectively. The term $\frac{3}{2} L_{fq} i_q$ represents the components of the field-linkage due to the quadrature mmf of the armature.

In the same manner as in Sec. 3.2, we have the inductances of field winding as follows:

$$\left.\begin{aligned} L_f &= \{ \sum_{n=1,3,5,\cdots} K_{fn} B_n (\sin n\eta_1 + \sin n\eta_2) \} / i_f \\ L_{fd} &= \{ \sum_{n=1,3,5,\cdots} K_{fn} B_{nd} (\sin n\eta_1 + \sin n\eta_2) \} \Big/ \left(-\frac{3}{2} i_d \right) \\ L_{fq} &= \{ \sum_{n=1,3,5,\cdots} K_{fn} B_{nq} (\cos n\eta_1 + \cos n\eta_2) \} \Big/ \left(-\frac{3}{2} i_q \right) \end{aligned}\right\} \tag{20}$$

It should be noted that L_{fq} implies a unilateral inductance from the armature to the field windings, and the field-linkage ψ_f consists of all stationary space harmonic components.

4. Experimental Results

4.1. Fundamental characteristics

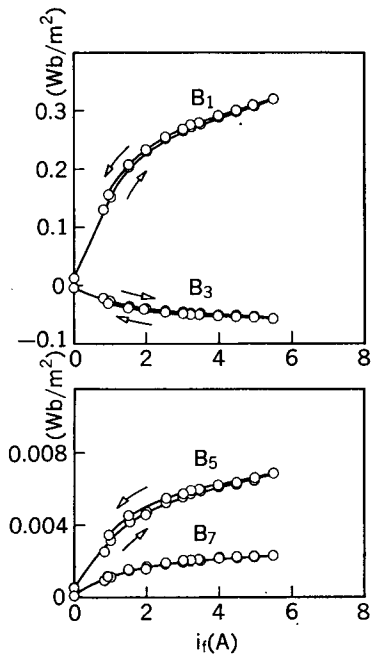

Fig. 7. No-load air-gap flux-densities.

Before giving the detailed experimental results, we show some fundamental characteristics of the tested generator and the experimental system.

Figure 7 shows the no-load air-gap flux-densities. The characteristic curves are little affected by the hysteresis of the core. It is needless to say that we only get the sum B_n+B_{nd} at the on-load test. When the separation of B_n or B_{nd} from B_n+B_{nd} becomes necessary, we use as B_n the lower values of the characteristics. The reason is merely to avoid the effect of hysteresis. This separation is due to the convenience for the treatment of experimental data. In fact, this separation criterion requires further detailed discussion correlated with the effect of saturation. However, we will not enter into this problem here.

Figure 8 shows the permanent three-phase short-circuit characteristics. From these results, the short circuit ratio of the tested generator turned out to be 2.00.

Figure 9 shows the steady-state stability region measured on the P, i_f plane for the system as shown in Fig. 2. As mentioned in Sec. 2.2, the measured points are marked by small circles in the figure. The hatched side in Fig. 9 shows the stable

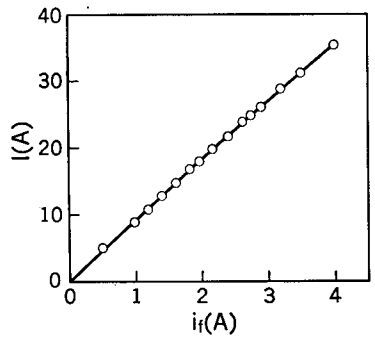

Fig. 8. Permanent three-phase short-circuit characteristics.

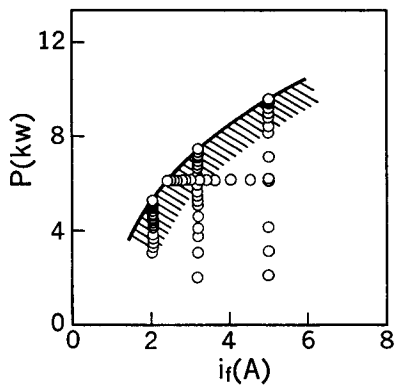

Fig. 9. Steady-state stability region.

region. When we bring P or i_f out of this region, the supplied mechanical input power to the generator cannot be converted into electric power, but accelerates the rotor velocity. Thus, the onset of asynchronization occurs[4].

4.2. Effective axial length and leakage impedance of armature windings

According to the procedure introduced in Sec. 3.3, the effective axial length l_e and leakage reactance x_{al} of the armature windings are evaluated. The results showed that the value of l_e is almost constant $l_e=0.147$(m)—$\kappa_e=1.13$—for all experimental conditions. On the other hand, the value of x_{al} depends on the operating conditions, and the results are shown in Fig. 10. We use the value $l_e=0.147$(m) in the following calculation of the inductances.

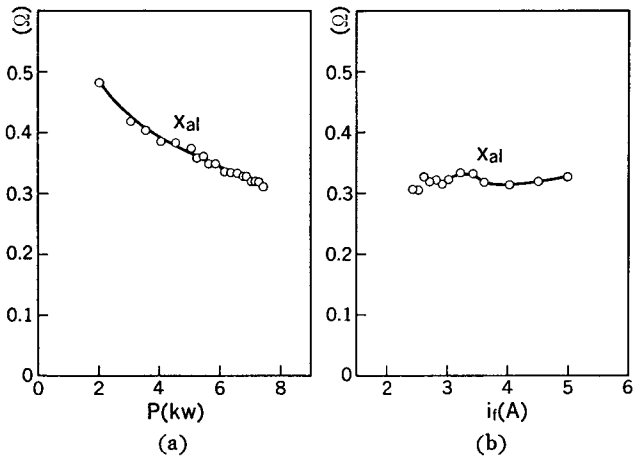

(a) x_{al} versus P with $i_f=3.2$(A)
(b) x_{al} versus i_f with $P=6.0$(kW)

Fig. 10. Appearances of leakage reactance.

4.3 Flux-based inductances

Let us begin by giving the experimental results concerning the terminal (phase) voltages, the armature currents and the air-gap flux-density distributions. Figure 11 shows these results for the case in which the output power P is increased by keeping the field current constant $i_f=3.2$(A). Similar tendencies to the results of Fig. 11 are observed for the different values of i_f. Figure 12 corresponds to the case in which i_f is decreased with $P=6.0$(kW).

Figures 13 and 14 give the values of inductances calculated by making use of such measured results as shown in Figs. 11 and 12. These results reveal the general aspects of inductances, which depend on the operating conditions of the synchronous generator. That is, the variations of the inductaces of armature windings are in general smaller than those of the field windings. Among the armature inductances, L_{aq} is almost constant but L_{ad}, L_{df} depend largely on i_f. As for the field induct-

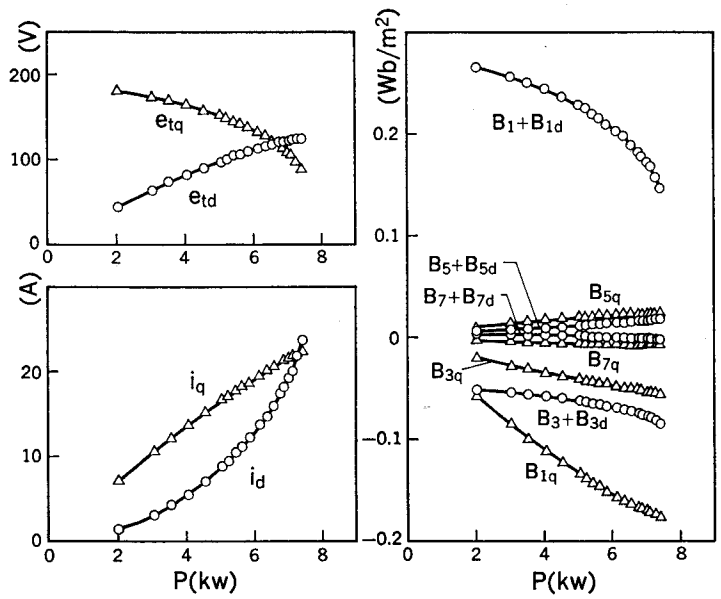

Fig. 11. Appearances of phase voltage, current and air-gap flux-density distribution for increasing P with $i_f=3.2$(A).

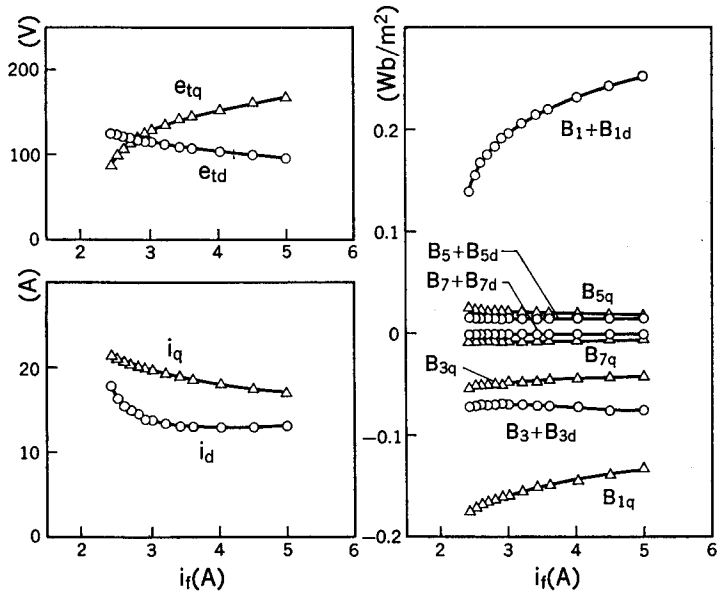

Fig. 12. Appearance of phase voltage, current and air-gap flux-density distribution for decreasing i_f with $P=6.0$(kW).

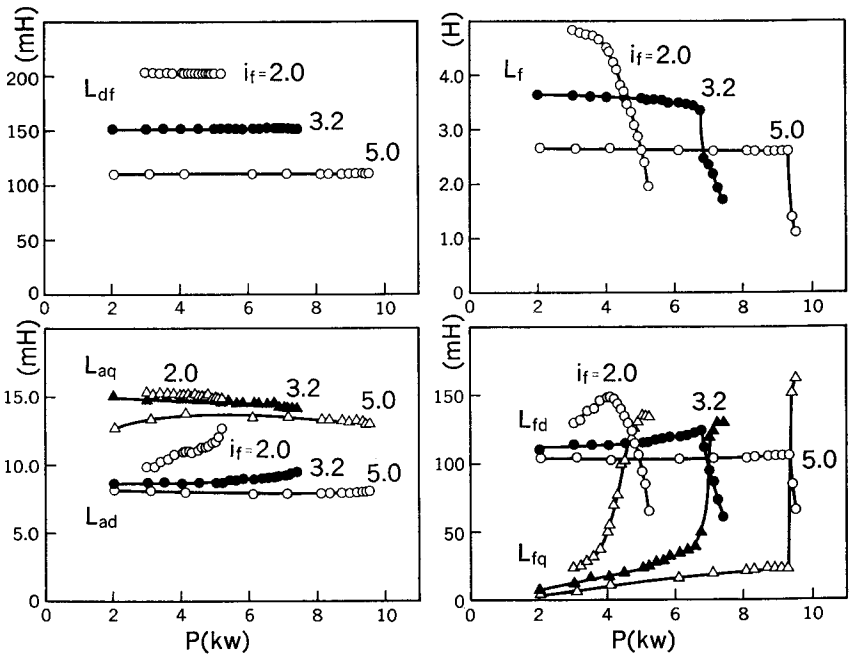

Fig. 13. Appearances of various inductances for increasing P with i_f=2.0, 3.2, 5.0(A).

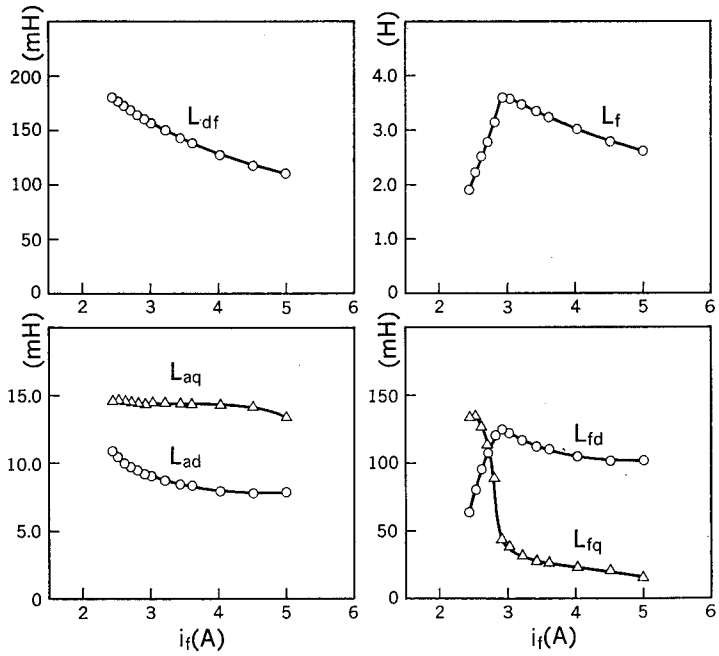

Fig. 14. Appearances of various inductances for decreasing i_f with P=6.0(kW).

ances, they undergo sudden changes at some operating conditions in the neighborhood of the steady-state stability limit. In particular, the appearance of L_{fq} is noteworthy.

5. Discussion

In the preceding section, we showed the flux-based inductances of the tested generator based on the actual state of the air-gap flux-density distributions. The results point out the new aspects of synchronous generator inductances which are inconsistent with conventional descriptions. Let us here discuss some of these subjects.

One of the distinctive features of the results is the appearance of L_{fq}. Though the tested generator has some special structures, the fact that L_{fq} is liable to appear for small i_f challenges the validity of the conventional derivation of the field flux-linkage ψ_f. Because the conventional derivations are based on the superposition of the flux components due to the field and the d-axis armature mmf. There is no room to take the q-axis armature mmf into account. However, as we see in Figs. 13 and 14, the appearance of L_{fq} for small i_f itself implies the counter evidences for the validity of superposition. In fact, magnetic saturation is not supposed to appear for a small field current.

Similarly, though the disagreement between L_{df} and L_{fd} is based on their definitions, this fact also deserves attention as material for further study.

The next subject to be discussed is the separation of B_n or B_{nd} from B_n+B_{nd}. Though the procedure used in the preceding section is due to the convenience of the data treatments, it is consistent with the conventional description. Taking into account the effect of magnetic saturation, this problem seems to be difficult when related with the long-pending problem of the calculation of field currents of synchronous generators. Even if we use a different criterion for the separation, the values of the inductances given in the preceding sections will be modified slightly, but their characters will remain unchanged.

The final subject concerns the relations between the flux-densities B_n, B_{nd}, B_{nq} and the currents i_f, i_d, i_q. This problem may fall under the category of the above subject. In the preceeding discussion, we suppose that B_n, B_{nd}, B_{nq} are mainly dependent only on i_f, i_d, i_q, respectively. At first sight this seems appropriate in a practical manner, but a detailed discussion will be required concerning the disputed points.

As mentioned above, the difficult problems are derived from the experimental facts. They are the roots of electro-magnetic dynamics but their clear explanations have not yet been made.

6. Conclusion

An experiment has been performed for the calculation of synchronous generator inductances based on air-gap flux-density distributions. As a result of this study, the general features of the inductances of the armature and the field windings have been made clear. In addition to these results, an alteration, Eq. (19), has been proposed for a conventional field flux-linkage relation. That is, the existence has been ascertained of unilateral inductance from the armature to the field windings, but the inductance cannot be derived from the conventional point of view. The physical conception of this inductance is supposed to represent some special features of rotating machines. However, the most important part of this subject remains to be held.

Acknowledgement

This research was supported by Grant-in-Aid of Scientific Research of the Ministry of Education, Science and Culture, Japan. It was also partly assisted by the Kansai Electric Power Co., Inc.

The authors wish to acknowlekge the cooperation for the experiment they received from Mr. Yoshitaka Miura, a former student of the Graduate School, Kyoto University.

References

1) For example: Concordia, C., "Synchoronous Machine", John Wiley & Sons Inc., New York, 1951.
2) Uenosono, C., Ueda, Y., Nanahara, T. and Kaneko, K., "Air-Gap Flux of a Synchronous Generator at Steady-State and Flux-Based Analysis of Generator Characteristics", Trans. I. E. E., Japan, Vol. 102-B, No. 5, pp. 281-288, May 1982, (English translation) Scripta, Vol. 102, No. 3, pp. 42-49, 1982.
3) Uenosono, C., Ueda, Y., Inoue, Y. and Hanai, T., "Armature Reaction of a Synchronous Generator on the Basis of Air-Gap Flux: Appearance of Instability in Case of Single Machine Operation", Trans. I. E. E., Japan, Vol. 102-B, No. 8, pp. 545-551, August 1982, (English translation) Scripta, Vol. 102, No. 4, pp. 115-121, 1982.
4) Ueda, Y., Hikihara, T. and Uenosono, C., "An Experimental Study on Dynamic Behavior of Magnetic Flux Distribution in a Synchronous Generator", Internationales Wissenshaftliches Kolloquium der Technischen Hochschule, Ilmenau, DDR, Oct. 29-Nov. 2, 1984.